Effect of Ball Burnishing on HCF of Bilayer Composite for Support Wind Turbine Blades

Yasser Fouad (yfouad@ksu.edu.sa)
King Saud University https://orcid.org/0000-0003-3797-4282
Haykel Marouani
King Saud University

Original Article

Keywords: High-cycle fatigue, Composite, Aluminum MMC, Al-Steel composite, Ball burnishing, wind blades

Posted Date: December 14th, 2020

DOI: https://doi.org/10.21203/rs.3.rs-122418/v1

Abstract

The cyclic deformation behavior of two metal-matrix composites, namely aluminum-based composites reinforced with a steel wire and aluminum-based composites reinforced with an aluminum alloy 3030 wire, was investigated at room temperature for wind blades support. All materials were synthesized by sand casting and subjected to mechanical surface treatment by ball burnishing. High cycle fatigue was observed under reversed bending loading at 50 Hz. The composites reinforced with volume fraction (28% and 34%) of the wire shows excellent fatigue life and endurance limit under stress-controlled conditions. Moreover, the tensile and microstructural properties of these materials were examined. The alloyed aluminum-matrix-steel-wire-reinforced composite showed higher fatigue behavior than the wire reinforced using ball burnishing of as-cast alloys.

Introduction

Aluminum metal matrix composites have higher specific strength and stiffness and excellent wear behavior, compared to aluminum alloys. luminum composites spasmodically fortified with material particulates have a mix of high specific strength and stiffness and low density. Achieving these properties were milestones toward using particulate-reinforced metal matrix composites (MMCs) in many applications due to their lower weight and greater stiffness. Many applications in manufacturing are based on cyclic loading during service, which causes fatigue degradation of the materials. In modern fields, Fatigue progress and behavior properties are basic factors in the plan of design parts. The cyclic deformation of MMCs is intricate and is emphatically influenced by many elements. These components include: (1) the matrix properties (e.g., chemical composition, structure, and heat treatment); (2) particulate-reinforcement phase properties (e.g., related to size, volume fraction, and bonding in the matrix); (3) test parameters (e.g., strain or stress control, type and frequency of loading, and temperature) and (4) processing routes [1–8]. Crack initiation in MMCs, is critically for fatigue life. Fatigue cracks start in unreinforced materials and are associated with slip band intrusions and extrusions on free surfaces [9–12]. The MMCs shows good fatigue at room temperature and endurance stress (related to their matrices) without being reinforced when exposed to HCF. More enhanced fatigue endurance of Al-MMCs than of aluminum only in fatigue and related to an increase in fatigue strength. Moreover, the stress controlled fatigue lives of Al-based MMCs have been reversible relation to particle size, and increased volume fraction within 0.7, and increased matrix tensile strength for a given stress level [13–14]. On the other hand, MMCs exhibit poorer low cycle fatigue (LCF) resistance compared to unreinforced metals under strain-controlled conditions. Low cycle fatigue life is related to low ductility of the composites with the result of ceramic reinforcements [15–17]. The materials used to reinforce Al alloys include carbides (e.g., SiC and TiC), zirconium boride (ZrB2), titanium diboride (TiB2), and oxides (Al2O3 and SiO2). Such reinforced Al alloys are particularly attractive because they exhibit high elastic modulus and hardness, good thermal stability, easy installation, and can be given directional control [18]. Reserachers shows two approaches by which to incorporate elements into Al-based alloys. The first approach involves wire reinforcing phases directly impeded within the matrix [19–20]. In this process, wire positions are formed

in flasks and then by casting Al-based alloys over the wire fixed during the casting process. A number of composites shows cleaner distribution of particle-matrix interfaces, so yielding strong interfacial surface-matrix bonding. These, fine with combined and uniform distribution of the wire within the matrices, means that the mechanical strength of such composites is enhanced considerably. The second approach involves the introduction of wire reinforcements into the matrices via ingot casting. The wire is synthesized separately or prior to composite fabrication.

Experimental Methods

An aluminum alloy and low-carbon-steel wire, 1 mm in diameter placed vertically within an alloy, and steel wires 0.5 mm diameter with 1 mm separation distance between the wires were used as base materials. Composites 1 and 2 Table 1. were prepared by sand casting as Y-blocks then machined to form cylinders, respectively. Machining of the produced cast alloys were performed to get the desired shapes for the mechanical testing samples and fatigue samples. The Al alloy was cast over the wire of steel or the wire as Y-block with diameter after machining of 5 mm. The chemical composition was determined using a Spectro Analytical instrument according to DIN 31051. The chemical composition of the materials is presented in Table 1. The materials were not heat treated; tensile and fatigue tests were applied directly. Fatigue test specimens were machined from the as-cast bars with the loading axis parallel to the wire direction. Shown in Fig. 1 the gauge length and diameter of the specimens were 14 and 6 mm. respectively. Fatigue tests were performed in a closed-loop servo hydraulic facility (Instron). Stress amplitude-controlled high cycle fatigue tests were conducted under bending force. Smooth specimens were cycled with a frequency of 50 Hz in ambient air at room temperature (20 °C). Fatigue life (Nf) was measured: 107 cycles was the limit of the test to establish a fatigue life (S-N) curve. Specimens were machined from as-cast materials. The specimens were ball-burnished (BB) to remove surface scratches. The ball burnishing condition was prepared using an ECOROLL instrument with HG6 tool type at 246 N with 0.17 mm/min feed rate at 30 rpm. Fatigue strength tests at the stress ratio (R) of − 1 were conducted with reversed bending loading techniques. The frequency was 50 Hz and the tests were done at room temperature (23 °C). A scanning electron microscope (HITACHI X-650) was used for examination of the surfaces. Micro-hardness tests were performed on surfaces containing the base metal and the reinforcement specimens. Tensile tests were performed on the alloys and composites.

Table 1
Chemical composition of Al 3030 and steel wire (wt %)

Al 3030	Al%	Zn%	Cu%	Fe%	Mn %	Ti%	Cr%	Si %	Sn %
	Balance	0.15	0.8	0.3	0.16	0.2	0.03	0.13	< 0.0752
	V%	Zr %	Mg%						
	0.0067	0.0057	0.02						
steel wire	Al%	Ca%	Cu%	Fe%	Mn %	Ni%	Pb %	Si %	Sn %
	78.8	0.0033	5.44	8.154	0.1811	0.2513	0.4503	5.25	< 0.0752
	V%	Zr %	Mg%						
	0.0067	0.0057	0.3069						

Results And Discussion

Figure 2. show the mechanical properties for all specimens, the amount will be showen in Table 2. Figures 3(a-h). Show the SEM fractography of composites 1 and 2. Reinforcement can be seen to impeded in the aluminum MC 1 in Fig. 3 (a–d). Steel alloy with substantial reinforcement is observed in the MMC Fig. 3e–h. Strengthening of reinforced particulate MMC is related to the parameters of the reinforcing particles, and also to the microstructure of the matrix. Cleavage of the reinforcement is related to large particulate size. Cracks or cavities were not initiated in alloys with limited steel reinforcement that impeded and bonded within the matrix. The mechanism of strengthening for reinforced MMCs was controlled by the mean diameter and volume fraction of the fine particles. The stress was related to the volume fraction of reinforcing particles, but inversely proportional to the particle diameter. Thus, composite 1 (steel wire with 0.34 volume fraction dispersed in an aluminum matrix) exhibited higher yield and tensile strength than did composite 2 (steel wire with 0.28 volume fraction). The microhardness of the surface results for samples before the fatigue tests were as follows for composite (1): average of 83 on HV scale for Al alloys and 238 for steel phase, while it was 200 at the interface area. The microhardness of composite (2) averaged 83 HV for the Al alloy and 230 for the steel phase, while it was 145 at the interface area. These were nearly the same for both composites. As stated before, the HCF resistance of reinforced particulate MMCs depends on many factors, volume fraction, particle size and microstructure of matrix, bonding between, tensile strength and the particle and matrix. The Al matrix may cause the formation of complex matrix microstructure, but it is easier to manufacture. Figure. 4, S-N curves show that the fatigue life of the composite (2) specimen which was less than that of composite (1), but both of them were longer than that of the matrix metal. The slope in the S-N curve was less in the composites with BB condition than in the Al alloys with BB condition. The ball burnishing process, sometimes called the deep rolling process, was very effective for increasing the service life and fatigue strength. It can be used for induced residual compressive stresses and work hardening of the surface layer to produce mirror-finish surfaces. A large difference exists in the fatigue life and fatigue limits,

especially at higher stress amplitudes. Insertion of elements via ball burnishing was performed with a hydrostatic ball with an inert drill hole, using a piston and screws with a torque of 4.9 N m. The best conditions for ball burnishing were produced by the best combination of pressure, feed rate, and speed. For the HG6 tool at 246 N, 30 rpm for Al composites was the best condition. Hardness for the MMCs was decreased from the circumference to the center, which indicated that the fatigue ratio was between 0.29 and 0.65 for as cast Al composite alloys, and the ratios were higher for alloys of greater strength. Here, the fatigue ratio for Al composites alloys at 10^7 cycles was 0.245. It was noticed that failure mainly started at the surface or slightly below the surface. This indicated that period of crack initiation may take up to 90% of the total fatigue life in a HCF regime; thus emphasis was put on the crack initiation mechanism. Fatigue failure leading to irreversible deformation could cause the concentration of local stress, leading to the initiation of cracks.

Table 2
Mechanical properties of investigated alloys.

Material	Proof stress 0.2% (MPa)	Tensile strength (MPa)	Elongation (%)	Young's modulus (GPa)
Composition (1) (steel wire) Vf = 34%	110.6	113.4	11.73	65
Composition (2) (steel wire) Vf = 28%	72.4	93.3	8.25	130

Conclusions

Fatigue tests and evaluation were performed using ball burnishing methods for Al- steel wires, wire alloy, and the base metal to elucidate if there were any effects from ball burnishing on the different combinations. The following conclusions were drawn:

1. Fatigue strength was increased in the case of steel wire reinforcement. Al base alloy fatigue life was low compared to other composites.
2. Fatigue behavior was improved by the metal matrix composite for all reinforcement types; fatigue life and endurance limits were remarkably increased, and this depended on the types of reinforcement and mechanical preparation route.
3. The improvement of fatigue behavior was due to steel reinforcement, which is considerably harder than the base alloy. For ball burnishing preparation, it is critical to choose the proper feed, speed, and tool head.
4. Cyclic failure was generated from the surface or near surface of specimens with the S-N curve exhibiting a continuous trend of decrease.

Declarations

ACKNOWLEDGMENTS

The authors extend their appreciation to the Deputyship for Research & Innovtion, Ministry of Education in Saudi Arabia for funding this reserch work through the project number (DRI-KSU-1410).

Authors' Contributions

Yasser Fouad was in charge of the whole trial and wrote the manuscript; H. Marouani was in charge of guidance and revision. All authors read and approved the final manuscript.

Funding

Supported by Deputyship for Research & Innovtion, Ministry of Education in Saudi Arabia for funding this reserch work through the project number (DRI-KSU-1410).

Competing Interests

The authors declare no competing financial interests.

References

1. Carreño-Morelli, E., Urreta, S. E., & Schaller, R. (2000). Mechanical spectroscopy of thermal stress relaxation at metal–ceramic interfaces in Aluminium-based composites. *Acta Materialia*, *48*(18–19), 4725–4733. https://doi.org/10.1016/s1359-6454(00)00264-0
2. Chawla, N., & Chawla, K. K. (2013). *Cyclic Fatigue*. 227–282. https://doi.org/10.1007/978-1-4614-9548-2_8
3. Daehn, G. (2000). *Thermal Cycling and Related Strain Mismatch in Metal Matrix Composites*. 419–445. https://doi.org/10.1016/b0-08-042993-9/00015-2
4. Fouad, Y. (2014). Characterization of High Strength Stainless Steel/Al/Brass Composite Tri-layered Clad. *Trans Indian Inst Met*, *67*(6), 979–988. https://doi.org/10.1007/s12666-014-0419-2
5. Fouad, Y., & Metwally, M. E. (2013). Shot-Peening Effect on High Cycling Fatigue of Al-Cu Alloy. *Metall and Mat Trans A*, *44*(12), 5488–5492. https://doi.org/10.1007/s11661-013-1899-0
6. Han, N. L., Yang, J.-M., & Wang, Z. G. (2000). Role of real matrix strain in low cycle fatigue life of a SiC particulate reinforced aluminum composite. *Scripta Materialia*, *43*(9), 801–805. https://doi.org/10.1016/s1359-6462(00)00492-9
7. Hassan, H. A., & Lewandowski, J. J. (2018). *4 Fracture Toughness and Fatigue of Particulate Metal Matrix Composites*. 86–136. https://doi.org/10.1016/b978-0-12-803581-8.09964-1

8. Huang, L., & Geng, L. (2017). *Microstructure Characteristics of Ti6Al4V Matrix Composites with Network Microstructure*. 39–55. https://doi.org/10.1007/978-981-10-4449-6_3
9. Ju, J. W., & Yanase, K. (2011a). Size-dependent Probabilistic Micromechanical Damage Mechanics for Particle-reinforced Metal Matrix Composites. *International Journal of Damage Mechanics*, *20*(7), 1021–1048. https://doi.org/10.1177/1056789510374165
10. Ju, J. W., & Yanase, K. (2011b). Size-dependent Probabilistic Micromechanical Damage Mechanics for Particle-reinforced Metal Matrix Composites. *International Journal of Damage Mechanics*, *20*(7), 1021–1048. https://doi.org/10.1177/1056789510374165
11. Madsen, B., Aslan, M., & Lilholt, H. (2016). Fractographic observations of the microstructural characteristics of flax fibre composites. *Composites Science and Technology*, *123*, 151–162. https://doi.org/10.1016/j.compscitech.2015.12.003
12. Mura, T. (1999). *A theory of fracture with a polygonal shape crack*. 3–15. https://doi.org/10.1016/b978-008043011-9/50002-8
13. Myriounis, D. P., Matikas, T. E., & Hasan, S. T. (2012). *Fatigue Behaviour of SiC Particulate-Reinforced A359 Aluminium Matrix Composites*. *48*(4), 333–341. https://doi.org/10.1111/j.1475-1305.2011.00827.x
14. Shanmughasundaram, P. (2014). Investigation on the Wear Behaviour of Eutectic Al-Si Alloy- Al2O3 - Graphite Composites Fabricated Through Squeeze Casting. *Res.*, *17*(4), 940–946. https://doi.org/10.1590/s1516-14392014005000088
15. Srivatsan, T. (1995). Cyclic strain resistance and fracture behaviour of Al2O3-particulate-reinforced 2014 aluminium alloy metal-matrix composites. *International Journal of Fatigue*, *17*(3), 183–199. https://doi.org/10.1016/0142-1123(95)98939-z
16. Srivatsan, T. S., Al-Hajri, M., Smith, C., & Petraroli, M. (2013). *Tensile Deformation and Fracture Characteristics of 2009 Aluminum Alloy Metal Matrix Composite*. 173–191. https://doi.org/10.1002/9781118787120.ch13
17. Srivatsan, T. S., Vasudevan, S., & Petraroli, M. (2008). The tensile deformation and fracture behavior of a magnesium alloy. *Journal of Alloys and Compounds*, *461*(1–2), 154–159. https://doi.org/10.1016/j.jallcom.2007.07.061
18. W. Albouy, B. Vieille, and L. Taleb, Composites Part A: (n.d.). *Applied Science and Manufacturing 67, 22 (2014).*
19. Wang, D., Shanthraj, P., Springer, H., & Raabe, D. (2018). Particle-induced damage in Fe–TiB2 high stiffness metal matrix composite steels. *Materials & Design*, *160*, 557–571. https://doi.org/10.1016/j.matdes.2018.09.033
20. Wang, J., Li, P., Chen, C., & Xue, J. (2012). *An In-Situ Technique for Preparing Al-TiB2 and Al-Al3Ti Composites*. 285–289. https://doi.org/10.1007/978-3-319-48179-1_49

Figures

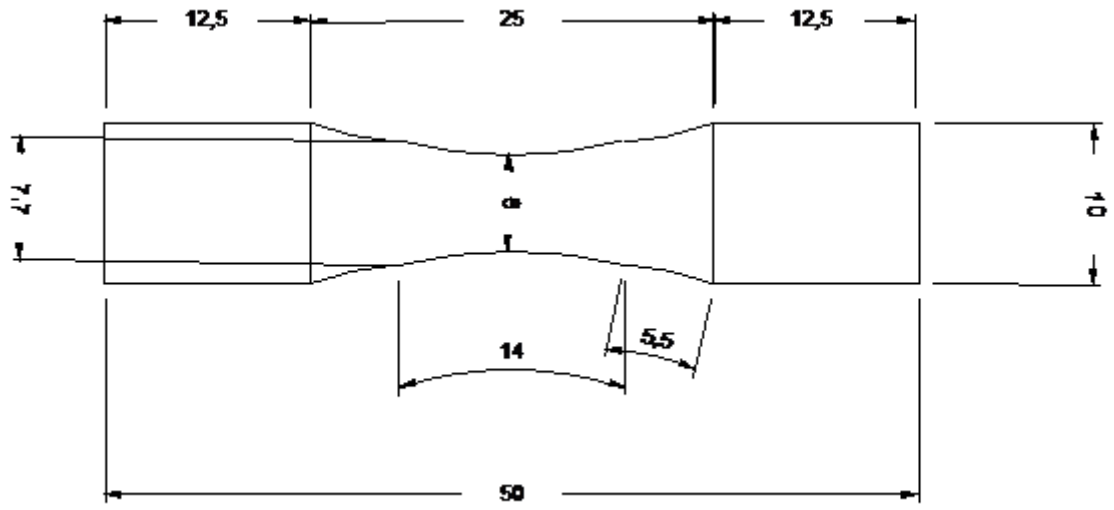

Figure 1

Shape and dimension of fatigue testing specimens

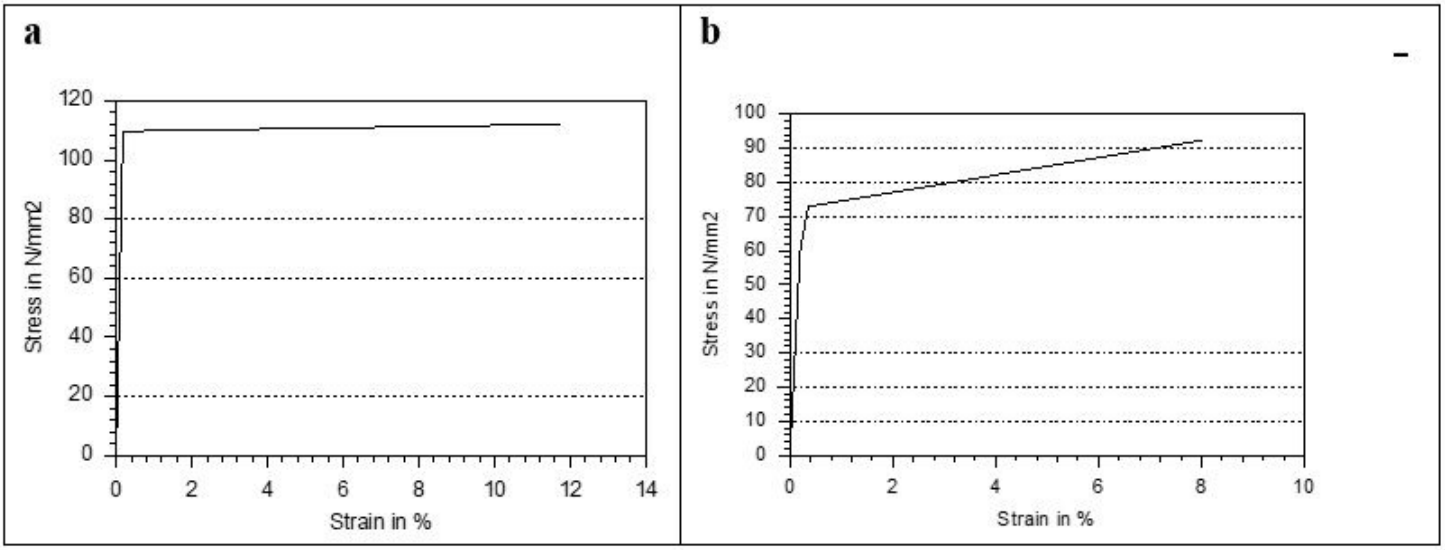

Figure 2

Stress – Strain diagram for (a) Al composite reinforcement with steel wire 1 (b) Al composite reinforcement with steel wire 2.

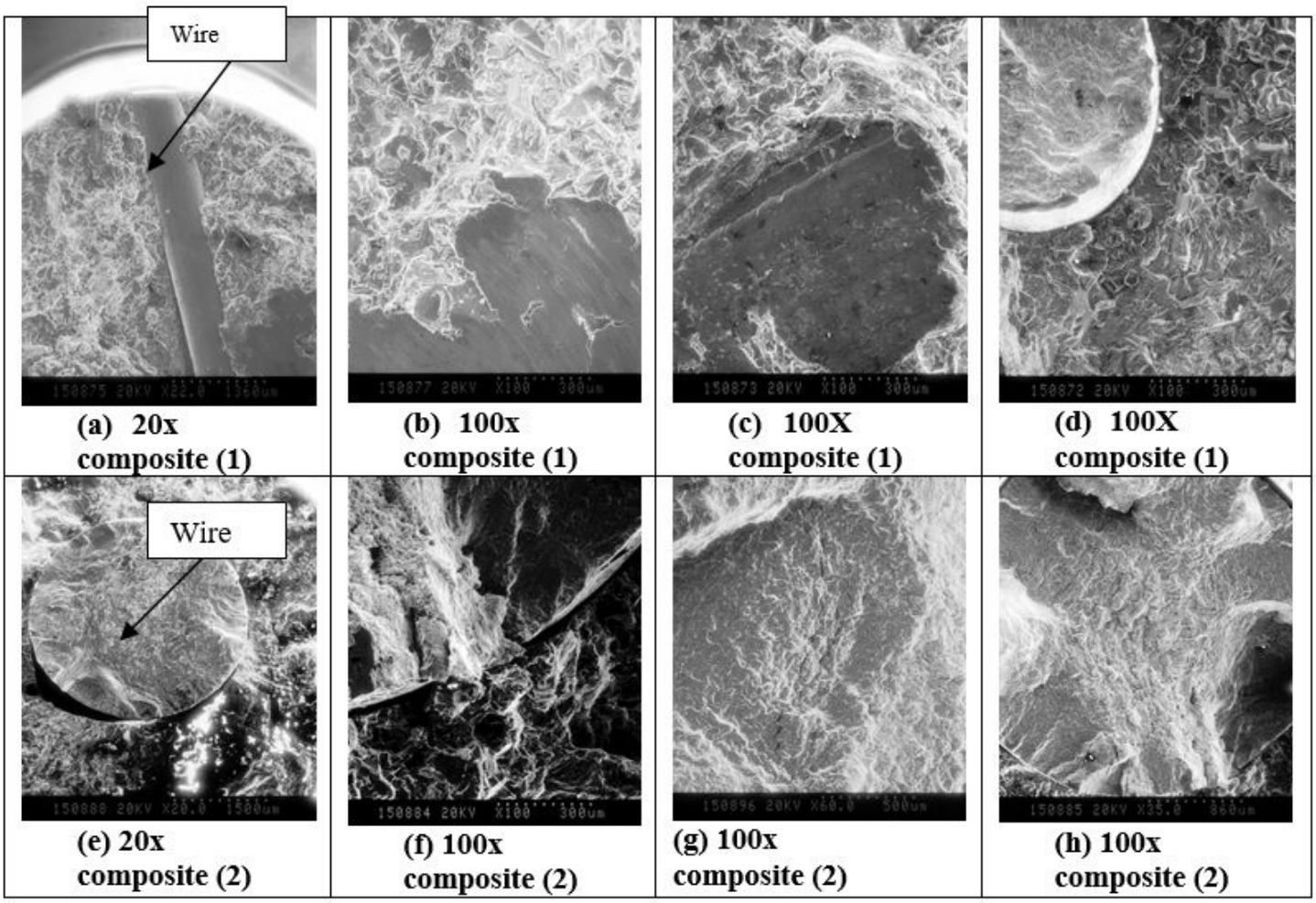

Figure 3

SEM Micrographs showing the microstructure of (a-d) of the as-cast Al –steel wire (e-h) and wire composites after Fatigue test.

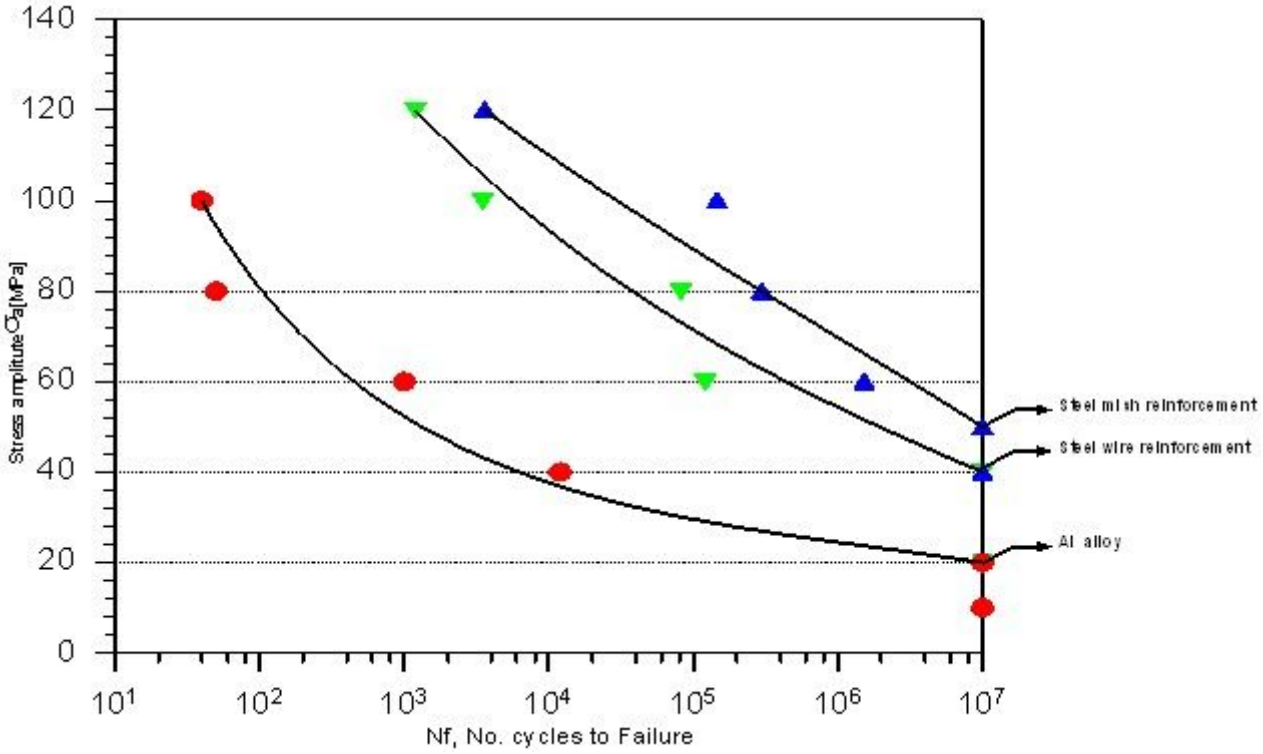

Figure 4

S-N curves of BB Al alloys and composites reinforcement by steel wire